

## Article

# Synthesis and Characterization of a Bioconjugate Based on Oleic Acid and L-Cysteine

Marco Vizcarra-Pacheco <sup>1</sup>, María Ley-Flores <sup>2</sup>, Ana Mizrahim Matrecitos-Burrueal <sup>3</sup>, Ricardo López-Esparza <sup>1</sup> , Daniel Fernández-Quiroz <sup>4</sup> , Armando Lucero-Acuña <sup>1,4</sup>  and Paul Zavala-Rivera <sup>1,4,\*</sup> 

<sup>1</sup> Departamento de Física, Universidad de Sonora, Blvd. Luis Encinas y Rosales S/N, Colonia Centro, 83000 Hermosillo, Sonora, Mexico; marco.vizcarra@unison.mx (M.V.-P.); ricardo.lopez@unison.mx (R.L.-E.); armando.lucero@unison.mx (A.L.-A.)

<sup>2</sup> Pritzker School of Molecular Engineering, The University of Chicago, Chicago, IL 60637, USA; mleyf@uchicago.edu

<sup>3</sup> Departamento de Investigación en Polímeros y Materiales, Universidad de Sonora, Av. Colosio S/N, Colonia Centro, 83000 Hermosillo, Sonora, Mexico; a213220985@unison.mx

<sup>4</sup> Departamento de Ingeniería Química y Metalurgia, Universidad de Sonora, Av. Colosio S/N, Colonia Centro, 83000 Hermosillo, Sonora, Mexico; daniel.fernandez@unison.mx

\* Correspondence: paul.zavala@unison.mx

**Abstract:** One of the main challenges facing materials science today is the synthesis of new biodegradable and biocompatible materials capable of improving existing ones. This work focused on the synthesis of new biomaterials from the bioconjugation of oleic acid with L-cysteine using carbodiimide. The resulting reaction leads to amide bonds between the carboxylic acid of oleic acid and the primary amine of L-cysteine. The formation of the bioconjugate was corroborated by Fourier transform infrared spectroscopy (FTIR), Raman spectroscopy, and nuclear magnetic resonance (NMR). In these techniques, the development of new materials with marked differences with the precursors was confirmed. Furthermore, NMR has elucidated a surfactant structure, with a hydrophilic part and a hydrophobic section. Ultraviolet-visible spectroscopy (UV-Vis) was used to determine the critical micellar concentration (CMC) of the bioconjugate. Subsequently, light diffraction (DLS) was used to analyze the size of the resulting self-assembled structures. Finally, transmission electron microscopy (TEM) was obtained, where the shape and size of the self-assembled structures were appreciated.

**Keywords:** surfactant; oleic acid; L-cysteine; bioconjugation; biomolecule



**Citation:** Vizcarra-Pacheco, M.; Ley-Flores, M.; Matrecitos-Burrueal, A.M.; López-Esparza, R.; Fernández-Quiroz, D.; Lucero-Acuña, A.; Zavala-Rivera, P. Synthesis and Characterization of a Bioconjugate Based on Oleic Acid and L-Cysteine. *Polymers* **2021**, *13*, 1791. <https://doi.org/10.3390/polym13111791>

Academic Editors: TriDung Ngo and Aman Ullah

Received: 13 March 2021

Accepted: 25 May 2021

Published: 29 May 2021

**Publisher's Note:** MDPI stays neutral with regard to jurisdictional claims in published maps and institutional affiliations.



**Copyright:** © 2021 by the authors. Licensee MDPI, Basel, Switzerland. This article is an open access article distributed under the terms and conditions of the Creative Commons Attribution (CC BY) license (<https://creativecommons.org/licenses/by/4.0/>).

## 1. Introduction

This work focused on the synthesis of new biomaterials from the bioconjugation of oleic acid with L-cysteine using carbodiimide. The process of chemically joining two or more molecules through a covalent bond with the help of a crosslinking agent is called bioconjugation. These agents have reactive ends for specific functional groups (primary amines, sulfhydryls, etc.) [1]. The demand for biocompatible and biodegradable materials for medical applications has increased the research of new compounds that satisfy those properties. Within these new compounds, some surfactants could meet these characteristics [2,3]. Surfactants have a characteristic molecular structure comprising a group (generally a long alkyl chain) with little attraction for the solvent (hydrophobic, if the solvent is water), together with another group (ionic or non-ionic) that shows a strong attraction of the solvent (hydrophilic in aqueous systems). The degree of surface activity and the type of application depends on the hydrophilic/lipophilic balance (HLB) characteristics of this amphiphilic structure [4]. The surfactant molecules of renewable raw materials that mimic natural lipoamino acids are one of the preferred options for food, pharmaceutical, and cosmetic applications [5]. These surfactants can be obtained from molecules that mimic natural amphiphilic structures. Based on these considerations, and as part of our study objective, a surfactant was synthesized from oleic acid and cysteine (lipoamino acids). The

association of polar amino acid and a non-polar long-chain compound to build amphiphilic structures allows obtaining molecules with a high surface activity [6]. When an amphiphilic molecule is dissolved, the lyophobic group distorts the structure of the solvent, increasing the free energy in the system [7]. The presence of an amino acid as a polar group in an amphiphilic molecule characterizes this type of surfactant. For its synthesis, amino acids used as protein building units, such as natural materials, are used. With the amino acids having a carboxylic group and a primary amino group, surfactants synthesized from them can be prepared by adding the hydrophobic component in either of the two parts, as presented in the literature [3].

Some studies indicate that amino acid-based surfactants form fibrillar structures are capable of gelling oils [8]. The nature of these fibers lies in the chiral self-assembly of amphiphilic molecules. The fibers form a three-dimensional network through the medium to form a gel. In general, the materials that exhibit these properties are referred to as low molecular weight gelling agents [9].

The amino acid can be derivatized by reacting to its carboxylate group with an alcohol to produce an aminated ester or with an amine to produce an amino amide. Alternatively, the amino group can be started by reacting it with a fatty acid to obtain an acidic amide or with an alkyl halide to form a secondary or tertiary amine, thus, producing an N-alkylaminoacid [2,3,5]. The term lipoamino acids apply to those compounds in which a single amino acid is linked, either through its carboxyl or amino group, to a long-chain fatty acid [10].

In 1909, S. Bondi synthesized lipoamino acids from glycine and alanine as N-lauroyl amino acids to elucidate the theory that fat necrosis in cells was attributed to the breakdown of acylamino acids into amino acids and fatty acids [11]. Later, in 1955, the natural existence of lipoamino acids was confirmed [12]. Since then, several lipoamino acids have been found in different living things [10].

In this work, L-cysteine was chosen because it contains a thiol group (-SH). The advantage of containing a thiol group is that sulfur in its different oxidation states represents one of the most versatile elements in molecular biology. Many of the sulfur compounds in living things, such as some vitamins, methionine, and cysteine, are essential for human nutrition by carrying out functions such as electron transport in Fe-S centers and structural roles through disulfide bridges [13]. Disulfide bridges in proteins improve the thermodynamic stability of the molecule and can be reversible in reducing environments. The reactivity of the individual cysteine thiols can be used to manipulate the oxidative assembly reactions [14,15]. These molecules are self-assembled due to London, Van der Waals dispersion forces, hydrogen bonds, and electrostatic and interfacial attraction and repulsion forces [8]. Besides, thiol groups are well known in nanotechnology for their property for self-assembly or self-organizing on specific metallic surfaces, like gold, silver, copper, among others.

The bioconjugation process involves the reaction between a carboxylic acid such as oleic acid with the amino group of an amino acid such as L-cysteine, forming an amide bond. However, the ideal method of amide synthesis by direct condensation of a carboxylic acid and an amine for the formation of an equivalent molecule of water as the sole by-product is not practical. As a result, activation of the acid component is necessary to promote amide coupling and develop an efficient synthesis process [16]. Like an alternative is used, the carbodiimide mediated conjugation, reported in 1955 [17]. For this type of conjugation, it is important to select carbodiimide based on the solvent, considering that a separation of the corresponding urea must occur. The case of reactions that start from fatty acids or a compound that is also soluble in non-polar or amphiphilic solvents, such as DMSO, should be used, and that the corresponding urea can be easily removed.

## 2. Materials and Methods

### 2.1. Materials

Oleic acid (natural, FCC), N-hydroxysuccinimide (98%), sodium hydroxide (ACS), dimethylsulfoxide (ACS), and hydrochloric acid (36.5–38%) were obtained from Sigma-Aldrich, St. Louis, MO, USA. L-cysteine (high purity grade) was obtained from Amresco, Pennsylvania, N,N'-dicyclohexylcarbodiimide of Alfa Aesar, Tewksbury, Massachusetts,). All materials were used without further modifications.

### 2.2. Methods

Preparation of amphiphilic molecules: For the formation of the final bioconjugate, a two-step synthesis system mediated by N'-dicyclohexylcarbodiimide (DCC) and N-hydroxysuccinimide (NHS) was carried out. This step corresponds to the formation of a stable ester from oleic acid by coupling carbodiimide with the carboxyl group of the acid, followed by its replacement by NHS. The next step corresponds to the nucleophilic attack of the primary amine of L-cysteine. The N-hydroxysuccinimide esters formed during the first stage have sufficient stability to allow a two-step reaction in which the conditions of the solution can be adjusted first to favor the formation of esters and subsequently adjusted to favor the amidation reaction [18], as show in Figure 1. The solvent used for the synthesis was DMSO.

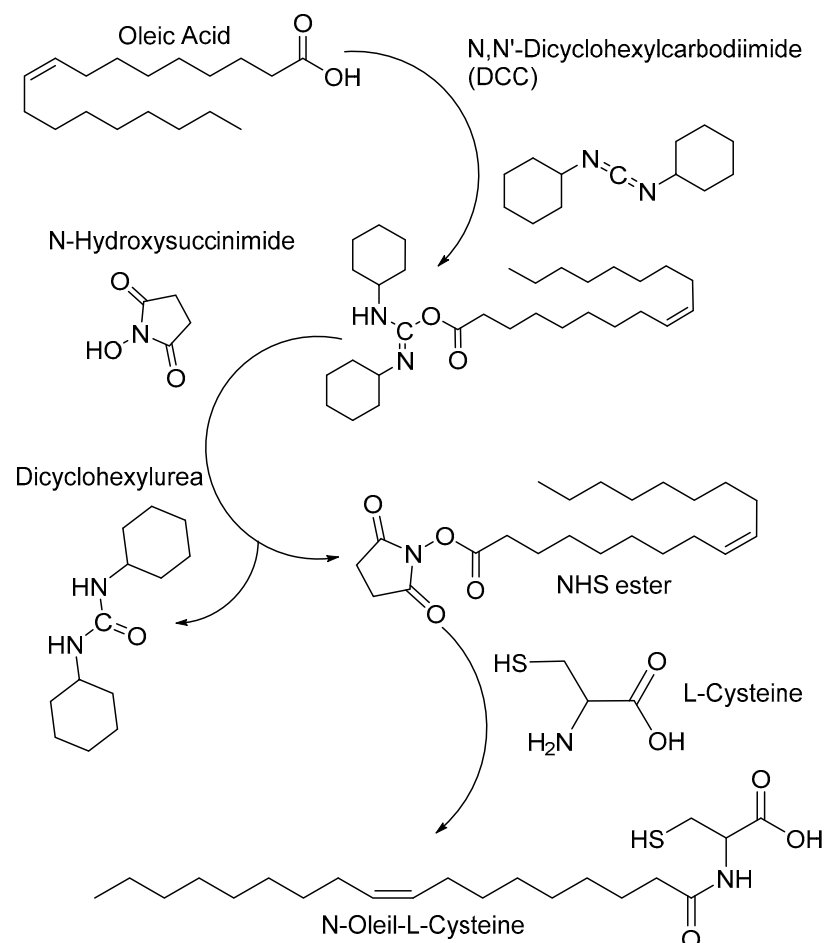


**Figure 1.** General scheme of the carbodiimide-based conjugation reaction for the synthesis of amphiphilic molecules of N-oleyl-L-cysteine.

Esterification of the oleic acid: 5 mL of a 0.002 M solution of Oleic acid, 5 mL of a 0.002 M solution of dicyclohexylcarbodiimide, and 5 mL of a 0.004 M solution of N-hydroxysuccinimide were prepared using a polar aprotic solvent such as dimethyl sul-

foxide as the medium of reaction. For the first step of the synthesis of lipoamino acid, the solutions of freshly prepared N-hydroxysuccinimide and dicyclohexylcarbodiimide were mixed in 5 mL of solvent. Due to the instability of O-acylisourea, the temperature decrease is suggested to increase the half-life of said molecule in solution [18]. For this reason, the solution was subjected to magnetic stirring in a cold bath at 10 °C to prevent the formation of N-oleylurea once the oleic acid is added. During this step, the protonation of the carbodiimide nitrogen facilitates the formation of the O-acylisourea because said protonation reduces the electron density in the central carbon of the carbodiimide, favoring the nucleophilic attack of the carbonyl group as shown in the literature [19]. Taking into account the above and considering that oleic acid has a pKa of 5.02, the solution of oleic acid was added, and the pH was lowered to 4 using a 0.1 M hydrochloric acid solution to promote the protonation necessary to the formation of the NHS-ester. In this step, the precipitation of dicyclohexylurea occurs as N-hydroxysuccinimide replaces the carbodiimide coupling, as reported in the literature.

**Amidation with L-cysteine:** The reaction of the N-hydroxysuccinimide ester with an amine is an example of a nucleophilic attack, for which the amine must remain deprotonated. After 15 min of stirring, the solution was adjusted to pH 9 using a solution of 1 M sodium hydroxide, and 0.0006 moles of L-cysteine was added directly. The reaction was left under stirring for 3 h and subsequently stored in a conical tube to precipitate the by-product corresponding to dicyclohexylurea and N-hydroxysuccinimide completely.

**Separation of reaction products:** The mixture was left to stand for 24 h, to induce the separation of the non-soluble undesired residues (mostly urea subproducts) by gravity. The supernatant was extracted using a micropipette and stored for further purification. A 4 mL sample was taken from the homogeneous solution to which 1 mL of a 0.3 M sodium hydroxide solution was added until a pH of 10 was reached to induce the formation of a gel; characteristic of amino acid-based surfactants [8]. The sample was left to rest for 24 h until complete gelification, then proceed to their separation from the rest of the reactant and residues left in liquid form. The route consisted of the direct extraction of the gel using tweezers, followed by two washes with deionized water, freeze-dried, and crushing the product with an agate mortar (Figure 2).

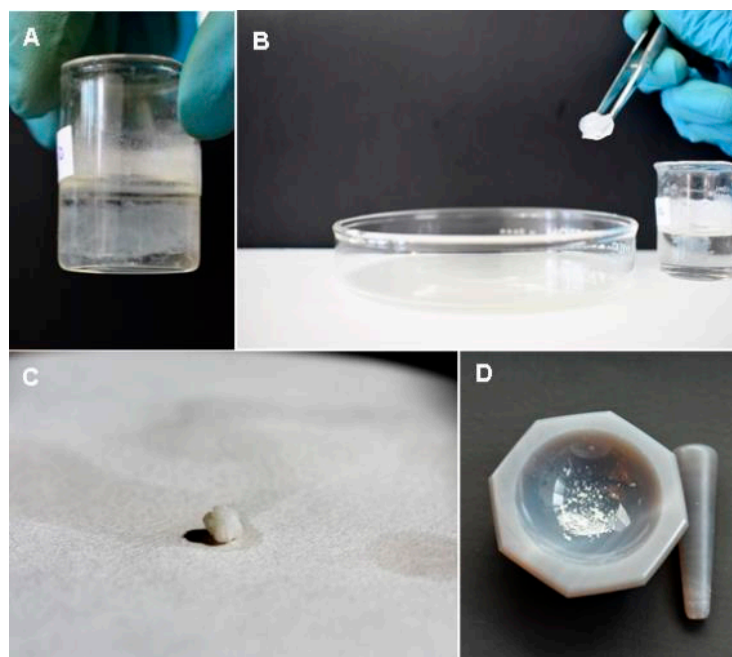


**Figure 2.** Process of separation of the bioconjugate of oleic acid and L. cysteine: (A) Formation of a gel at pH 12, (B) Physical extraction of the gel, (C) Drying, and (D) Crushing of the sample.

### 2.3. Characterization Techniques

The dry form obtained by gelation was used for the characterization techniques herein described. High-resolution  $^1\text{H-NMR}$  spectroscopy was recorded on a Bruker Avance 400 spectrometer operating at 400 MHz. The sample was solubilized in DMSO- $d_6$  (99.9 atom % D) using TMS as an internal reference. For FTIR spectroscopy, the spectral data were obtained using a Thermo Scientific brand spectrometer model Nicolet iS50, the samples were dry and placed directly on the diamond window of the ATR mode (attenuated total reflectance), and the spectrum was measured in a range between 4000 and 500  $\text{cm}^{-1}$  (64 scans per sample). For Raman spectroscopy, experiments were performed at room temperature using a 473 nm diode laser (Excelsior One 473, Spectra-Physics, MKS Instruments, Inc, Santa Clara, California, CA, USA) with an incident power of about 5.0 mW. The light was focused and collected with a 100 $\times$  objective. The emitted light was detected with a 0.55 m spectrometer (iHR550, Horiba, Miyanohigashi, Japan) and a cooled CCD (CCD-1024x256-BD-SYN, Horiba). The elastic component of the collected light was removed by a Notch filter. DLS experiments were done using a Brookhaven BI-200SM Research Goniometer System with a 637 nm He-Ne laser and 15 mW power. The intensity correlation function was measured at a fixed angle of 90 degrees. UV-visible spectrophotometry was performed with the VWR brand double beam spectrophotometer; model UV-6300PC with UV-Visible scanning. This technique was used to determine the critical micellar concentration (CMC) value roughly, whereas a micellar solution acts as a colloidal suspension relative to the wavelength of light [20]. This method is based on the change in absorption behavior after aggregation [21]. For transmission electron microscopy (TEM), a JEOL JEM-2010F field emission apparatus (Akishima-shi, Japan) was used, operating at 200 keV on a 200-mesh carbon on a copper grid (Ted Pella) followed by a drop of 3% phosphotungstic acid as a staining agent. Micrographs were taken and analyzed using Gatan software (Gatan Inc., Pleasanton, CA, USA).

### 3. Results

Nuclear magnetic resonance characterization: The  $^1\text{H-NMR}$  spectrum of *N*-oleyl-L-cysteine bioconjugate (MAT) is presented in Figure 3. The signal corresponding to the methyl protons was found at  $\delta\text{H} = 0.85$  (a), followed by the signals corresponding to the alkyl protons  $\text{CH}_2$  of the oleic acid chain  $\delta\text{H} = 1.29\text{--}1.20$  (b). The protons of the methylene group were found in  $\delta\text{H} = 5.32$  (d), and the most immediate carbon protons to this were found at  $\delta\text{H} = 1.97$  (c). Because deuterated DMSO was used as a solvent for this experiment, a representative substitution of the hydroxyl group and amide group protons was not observed. Therefore, the proton signal of the hydroxyl group was found in  $\delta\text{H} = 10.35$  (h) and  $\delta\text{H} = 6.96\text{--}7.22$  (g) the signals of the protons corresponding to the three amide groups found in the synthesized molecule were found [22]. The characteristic proton signals and integrals were suggestive of bioconjugate formation, and the proposed structure is shown inside (Figure 3).

The spectrum presented in Figure 3 corresponds to the purified bioconjugate, but the signals of some reaction impurities were observed. In this sense, the signals at  $\delta\text{H} = 1.58\text{--}1.73$  are associated with the alkyl protons of the cyclohexyl rings of the *N*-acyl urea, which is a secondary reaction product. Similarly, it is identified at  $\delta\text{H} = 5.59$ , the nitrogen proton in the urea group [23].

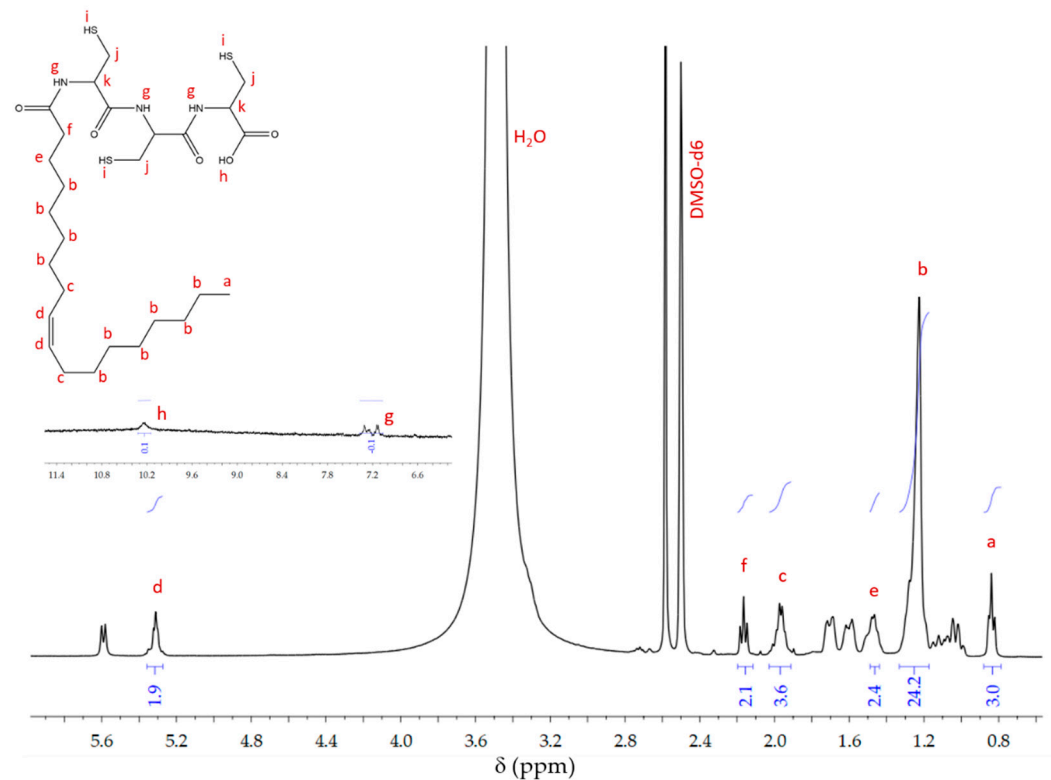


**Figure 3.**  $^1\text{H-NMR}$  spectrum of (MAT).

Infrared spectroscopy: In the spectrum corresponding to oleic acid (OA). We can observe in  $3005\text{ cm}^{-1}$  the signal corresponding to the stretching of the C–H bond adjacent to its unsaturation. We also found two very marked bands in  $2921$  and  $2852\text{ cm}^{-1}$ , corresponding to the asymmetric and symmetrical stretches, respectively, of C–H of the alkyl chain. In  $1707\text{ cm}^{-1}$ , was found the characteristic band of the carbonyl group present in said fatty acid corresponding to the C=O stretching of the carbonyl. Moreover, in the spectrum for L-cysteine (CYS), we observe in  $3163\text{ cm}^{-1}$  the representative band of the N–H stretch of the amino group, the characteristic vibrations of the thiol group S–H can be observed in  $2550\text{ cm}^{-1}$ , and the C–S link appears in the  $635\text{ cm}^{-1}$  [15,24,25]. Finally, the spectrum for the oleic acid and L-cysteine bioconjugate (MAT) was obtained from a solid-state sample. Comparing the spectrum of the bioconjugate with that of L-cysteine, the following bands were found. First, at  $3320\text{ cm}^{-1}$ , the first difference for the spectrum compared to the L-cysteine spectrum, which corresponds to the N–H stretching vibration of the amide group. At  $2580\text{ cm}^{-1}$ , the associated band of the S–H from the thiol group was found shifted from the earlier band at  $2543\text{ cm}^{-1}$  present in the molecule. The carbonyl group C=O is observed in  $1705\text{ cm}^{-1}$ . In  $1624\text{ cm}^{-1}$ , a new band corresponding to the vibration of the carbonyl group set called amide appears, In addition, carboxylic acids show characteristic C–O stretching in  $1240\text{ cm}^{-1}$ . Besides, the band corresponding to the C–S link is pronounced in  $643\text{ cm}^{-1}$ , indicating a strong presence of this link in the product formed [24–27] (Figure 4).

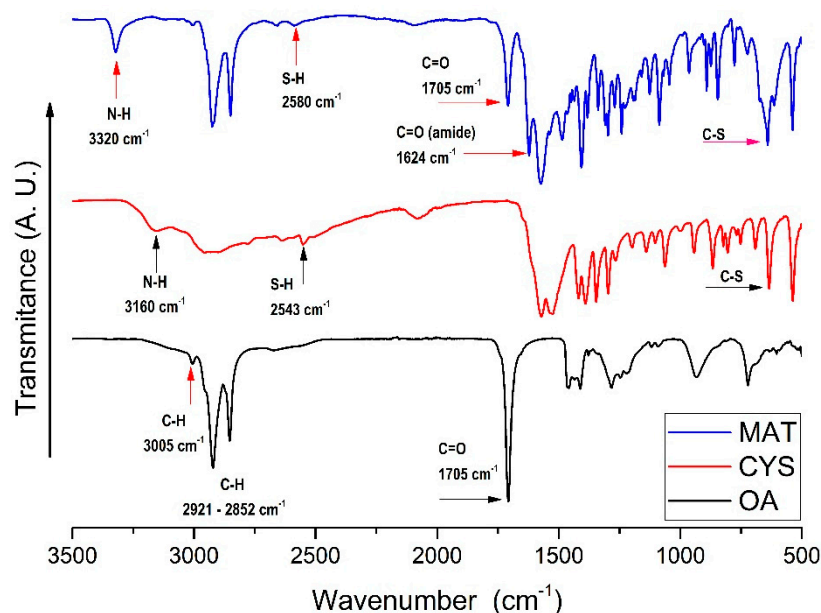


**Figure 4.** Infrared spectra; Oleic acid (OA), L-cysteine (CYS), and (C) Bioconjugate of oleic acid and L-cysteine (MAT).

The Raman spectroscopy: The spectrum of L-cysteine shows signals associated with its chemical structure, in the region of 200 to 500  $\text{cm}^{-1}$ , the ones associated with the vibrations of CCC bend, CCC rock, CCN bend, and CCS bend [28]. Moreover, the signal at 640  $\text{cm}^{-1}$  corresponds to the stretching vibrations of the CS link. The peak observed in 2544  $\text{cm}^{-1}$  corresponds to the HS link of mercaptan [29]. Regarding the Raman spectroscopy of oleic acid, the literature establishes the peaks of 1000–1200 and 2800–3000  $\text{cm}^{-1}$ , which are indicators of the torsion and packing signal, respectively, of the chain. As well as signals in the region of 2850 and 2930  $\text{cm}^{-1}$  corresponding to the vibrational modes of asymmetric  $\text{CH}_2$  and symmetric  $\text{CH}_3$ , respectively, and sensitive to hydrophobic interactions between hydrocarbon chains and indicate chain packing [30].

In the spectrum analysis, we found in 720  $\text{cm}^{-1}$  the signal of the thiol SH group, corresponding to a stretch in phase; later, we observed the signal of the  $\text{CH}_2$  group corresponding to the aliphatic chain of oleic acid in 731  $\text{cm}^{-1}$  of the rock movement in phase; in 1417  $\text{cm}^{-1}$  the CH signal appears, the C–NH link of stretching and bending appears in 1551  $\text{cm}^{-1}$ , the double bond of carbon–carbon we see in 1660  $\text{cm}^{-1}$ , assigned to stretching, the carbonyl group appears in 1751  $\text{cm}^{-1}$ , assigned to stretching in phase. The signal of the NH group of the amide is observed at 2327  $\text{cm}^{-1}$ , which confirms the presence of the peptide bond. Subsequently, a broad band appears, in which some signals such as the fermi resonance of  $\text{CH}_2$  in 2890  $\text{cm}^{-1}$  are combined, the overtone of the C–NH bond in 2943  $\text{cm}^{-1}$ , and the signal of a  $\text{CH}_3$ , of the oleic acid chain. Furthermore, an O–H stretch band around 3428  $\text{cm}^{-1}$  in the Raman spectrum of (MAT) is indicative of carboxylic acid groups on L-cysteine [29] (Figure 5).

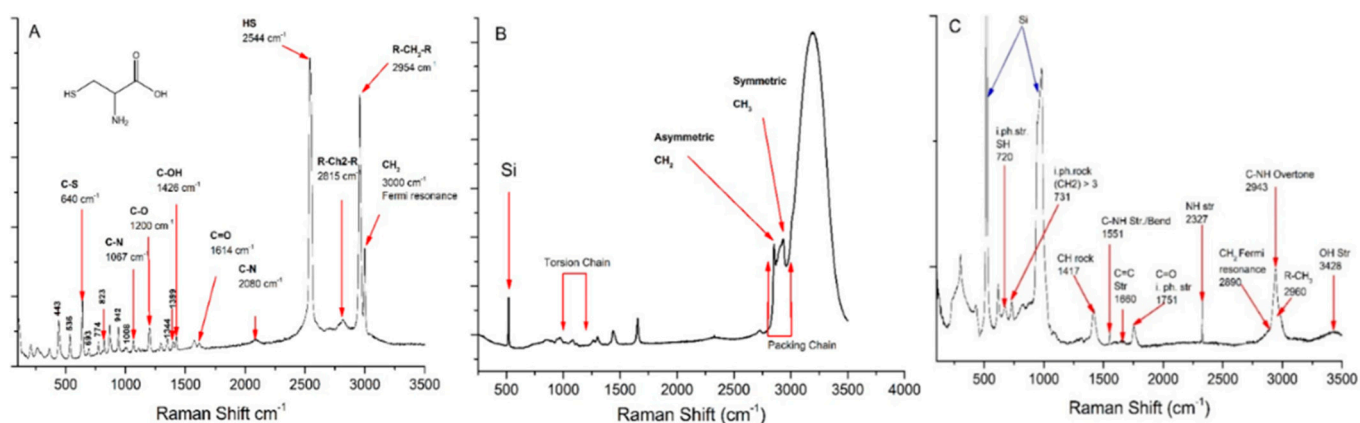


**Figure 5.** Raman spectra. (A) Amino acid L-cysteine. (B) Oleic acid, (C) bioconjugated material of oleic acid and L-cysteine (MAT).

**Critical micellar concentration (CMC):** The critical micellar concentration of a surfactant solution can be easily determined by plotting the absorbance as a function of surfactant concentration. The cross intersection between the two slopes is taken as the CMC of that solution. The interaction between solute–solute molecules and solute–solvent molecules can give useful information about the interfacial and thermodynamic properties. These behaviors are attributed to the delicate balance between the hydrophobic and hydrophilic interaction of the surfactant solution [20]. The different concentrations of the surfactant were analyzed using a quartz cuvette at different concentrations of MAT in deionized water.

By applying the UV-Vis technique, the CMC of a new material was determined, a solution with 0.0012 g of MAT in solid state was prepared and dissolved in 0.002 L of deionized water, which is equivalent to a concentration of 0.600 g/L. This concentration marked the beginning of UV-Vis measurements (Figure 6). The wavelength used was 204 nm, which corresponds to the length at which cysteine is absorbed. The value determined for CMC = 0.226 g/L. This value is considered approximate to the actual value of CMC.

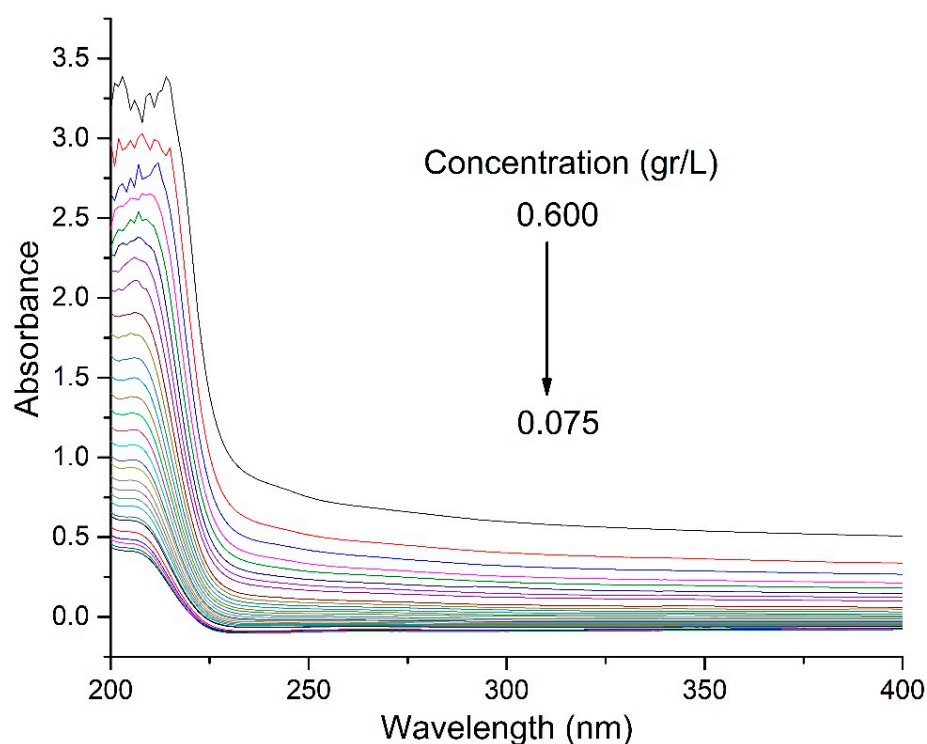


**Figure 6.** UV-Vis spectrum of bioconjugate of oleic acid and L-cysteine (MAT).

The CMC was determined by plotting the absorbance against concentration. The graph presents two parts with different slopes, and the CMC was evaluated from their point of intersection. The CMC values obtained from the given UV-Visible data are shown in Figure 7.

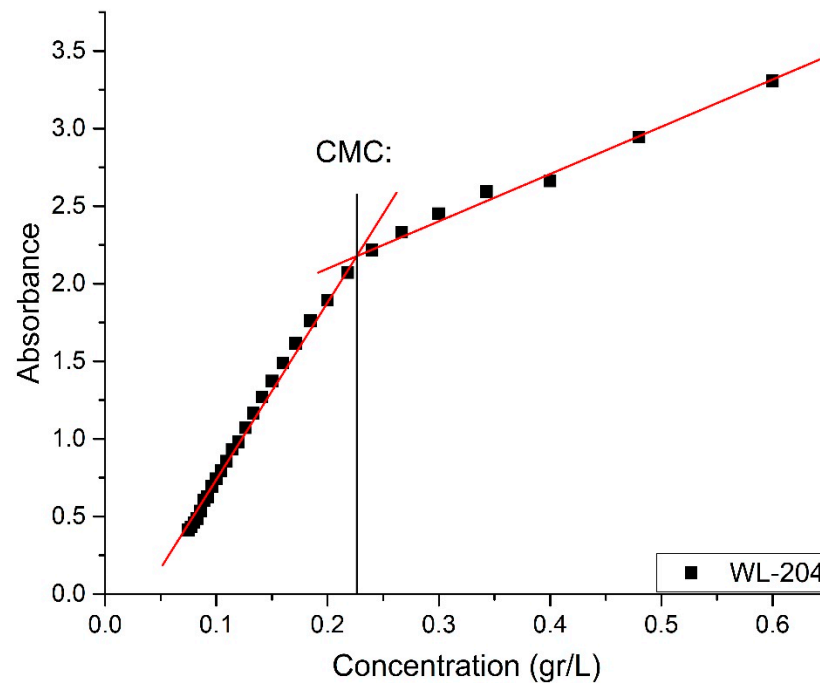


**Figure 7.** Absorbance versus concentration plots of bioconjugate of oleic acid and L-cysteine (MAT). Wavelength 204 nm.

Dynamic scattering of light (DLS): To determine the hydrodynamic ratio of the particle, dynamic light scattering experiments (DLS) were performed. A dynamic light scattering experiment consists of having a laser beam effect sample and collecting the light scattered at an angle  $\theta$  with a photomultiplier. The intensity fluctuations of the scattered light allow obtaining the normalized correlation function.

$$g_2(\tau) - 1 = B|g_1(\tau)|^2$$

where  $\tau$  is the characteristic time of the decay of the correlation and  $B$  is a parameter that depends on the experimental geometry. In the case of a monodisperse solution, the field correlation function decays as  $g_1(\tau) = \exp(-\Gamma t)$  with a decay given by  $\Gamma = Dq^2$  where  $D$  is the mutual diffusion coefficient and  $q = \frac{4\pi n}{\lambda} \sin\left(\frac{\theta}{2}\right)$  is the magnitude of the scattering vector,  $n$  the refractive index,  $\lambda$  the wavelength, and  $\theta$  the scattering angle.

Two samples were measured, the first one at a CMC concentration obtained by UV-Vis (0.226 g/L) as shown in Figure 7; only noise was detected, and a hydrodynamic radius could not be established. The second sample was used at a concentration above the CMC calculated at 0.3 g/L.

The sample cells were 2-mL cylindrical ampoules (concentration = 0.3 g/L) immersed in an index-matching bath of decline, thermostat at 25 °C. The sample was filtered and sonicated for 10 min, before measurements.  $\Gamma$  was obtained by adjusting the correlation function for a decaying exponential and was used in the Stoke–Einstein equation.

$$D = \frac{k_B T}{6\pi\eta R}$$

where  $R$  is the hydrodynamic radius,  $k_B$  is Boltzmann's constant,  $T$  is the temperature, and  $\eta$  is the viscosity of the solvent. The value obtained for the hydrodynamic radius is 50.57 nm, and the polydispersity index (PDI) is 0.1602 (Figures 8 and 9).

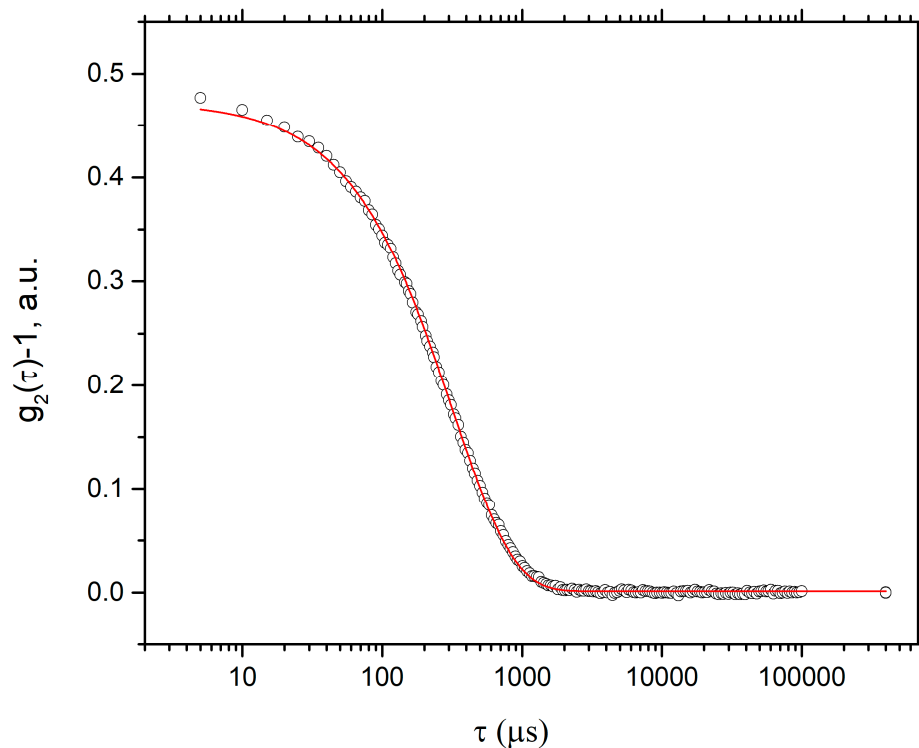


**Figure 8.** Correlation curve obtained by DLS of the MAT sample at 0.3 g/L at 25 °C.

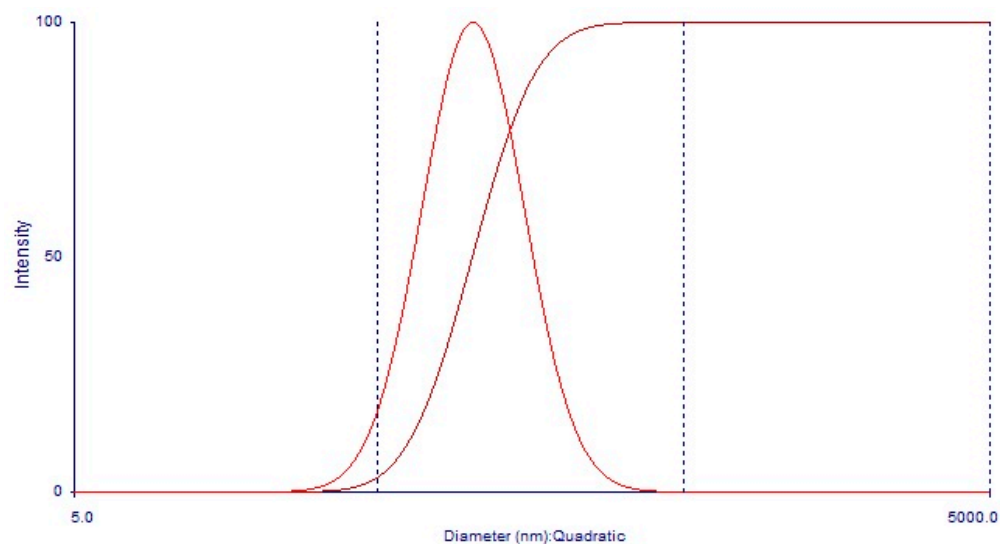


**Figure 9.** Hydrodynamic diameter distribution of 101.14 nm of the MAT sample at 0.3 g/L by DLS.

Transmission Electron Microscopy (TEM): The morphology observed in the micrographs shows spherical and cylindrical shapes (Figure 10). The average particle radius value found is 31.81 nm obtained using ImageJ 1.51m9 software from Wayne Rasband, National Institute of Health (500 particles analyzed), presented in Figure 11.

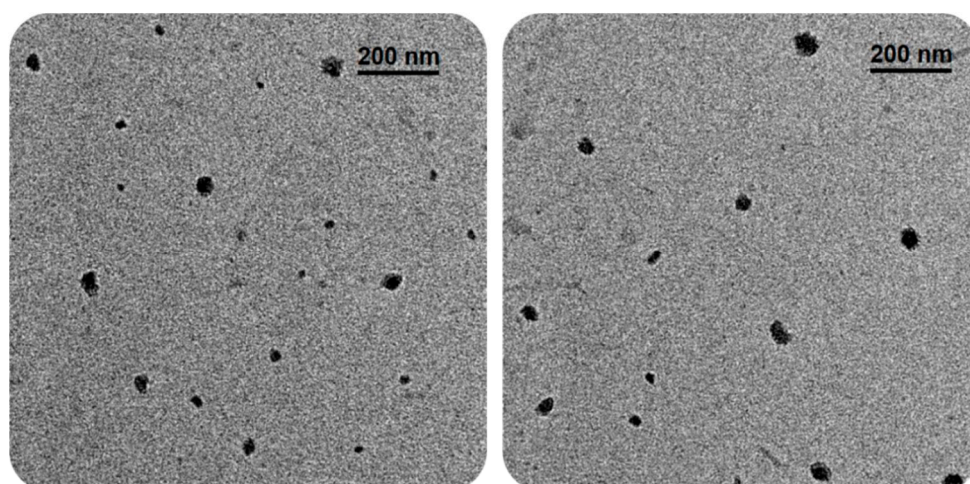


Figure 10. TEM images show spherical and cylindrical particles and sizes less than 100 nm.

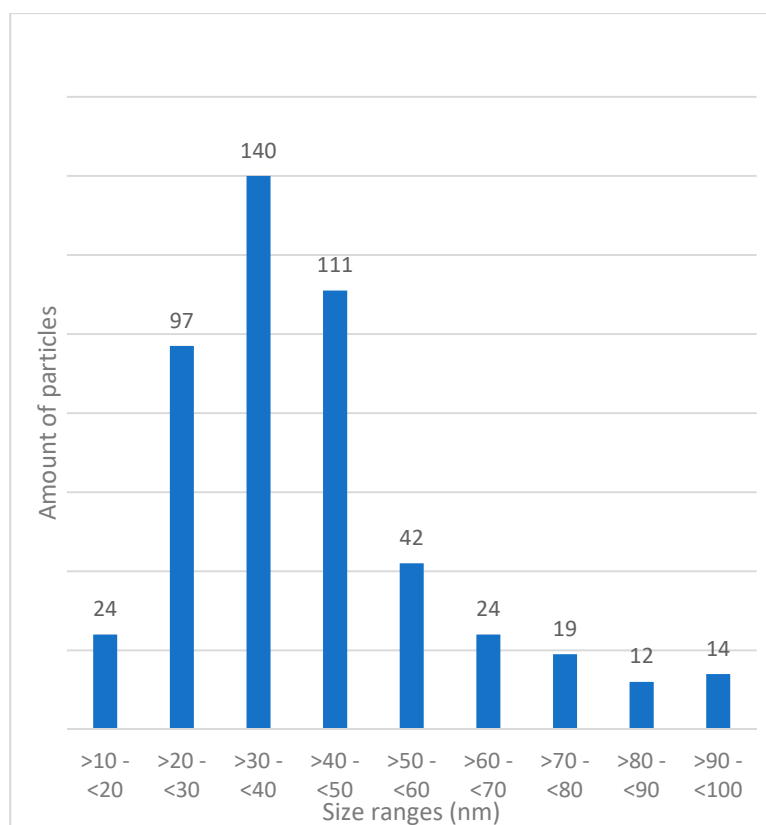


Figure 11. Histogram of sizes obtained in TEM. On the X-axis, we have size ranges (nm), and on the Y-axis, we have the number of particles.

The values TEM using a JEOL JEM-2010F Field Emission apparatus (Akishima-shi, Japan) operating at 200 keV on a 200-mesh carbon on a copper grid (Ted Pella) followed by a drop of 3% phosphotungstic acid staining agent. Micrographs were taken and analyzed using Gatan software (Gatan Inc., Pleasanton, CA, USA).

#### 4. Conclusions

In this work, we sought to obtain a bioconjugate of L-cysteine and oleic acid through a coupling reaction assisted by carbodiimide.  $^1\text{H-NMR}$  spectroscopy was employed to elucidate a molecule of the bioconjugate material; the signals and integrals characteristics

of the protons suggested the formation of a molecule formed by one oleic acid molecule and three molecules of cysteine. Infrared spectroscopy confirmed the formation of an amide group that resulted from the coupling reaction and suggested that for the synthesis conditions used, there were no disulfide bridges. An approximate value of the micellar critical concentration (CMC) was obtained using UV-Vis and TEM confirms self-assembling structures of spherical and cylindrical shapes with an average size radius of 31.81 nm; comparable to the 50.57 nm of hydrodynamic radius obtained by DLS. In addition, the study is underway to explore the possible applications, within which we could include that of encapsulant of bioactive molecules with hydrophobic properties or as surface modification of gold, silver, or any other metal, reactive to thiol groups nanoparticles.

## 5. Patents

This research has been submitted for a licensed patent in Mexico with the file number MX/a/2018/016047, dated 12 December 2018.

**Author Contributions:** Experiments and article editing were realized by M.V.-P., M.L.-F., and A.M.M.-B.; Discussions and characterization by P.Z.-R., A.L.-A., D.F.-Q., and R.L.-E.; Experimental design, interpretation of results and article written by P.Z.-R. and A.L.-A. All authors have read and agreed to the published version of the manuscript.

**Funding:** The APC was funded by Consejo Nacional de Ciencia y Tecnología (CONACYT) from Mexico through the National Graduate Scholarship Programs.

**Institutional Review Board Statement:** Not applicable.

**Informed Consent Statement:** Not applicable.

**Data Availability Statement:** The data presented in this study are available on request from the corresponding author.

**Acknowledgments:** We acknowledge Susana Álvarez from the “Physics Research Department” at the University of Sonora for helping us with the characterizations in the Raman equipment. We are grateful for the use of the transmission electron microscopy (TEM) facilities of the University of Sonora, and we thank Refugio Pérez-González and Ramón Moreno of the Spectroscopy Laboratory of the Department of Polymers and Materials of the University of Sonora for providing the <sup>1</sup>H-NMR spectra.

**Conflicts of Interest:** The authors declare no conflict of interest.

## References

1. Thermo Scientific. *Crosslinking Technology Handbook*; Thermo Fisher Scientific Inc.: Waltham, MA, USA, 2012.
2. Infante, M.R.; Pérez, L.; Pinazo, A.; Clapés, P.; Morán, M.C.; Angelet, M.; García, M.T.; Vinardell, M.P. Amino acid-based surfactants. *C. R. Chim.* **2004**, *7*, 583–592. [[CrossRef](#)]
3. Bordes, R.; Holmberg, K. Amino acid-based surfactants—Do they deserve more attention? *Adv. Colloid Interface Sci.* **2015**, *222*, 79–91. [[CrossRef](#)] [[PubMed](#)]
4. Macián, M.; Seguer, J.; Infante, M.R.; Selve, C.; Vinardell, M.P. Preliminary studies of the toxic effects of non-ionic surfactants derived from lysine. *Toxicology* **1996**, *106*, 1–9. [[CrossRef](#)]
5. Morán, M.C.; Pinazo, A.; Pérez, L.; Clapés, P.; Angelet, M.; García, M.T.; Vinardell, M.P.; Infante, M.R. “Green” amino acid-based surfactants. *Green Chem.* **2004**, *6*, 233–240. [[CrossRef](#)]
6. Rondel, C.; Alric, I.; Mouloungui, Z.; Blanco, J.F.; Silvestre, F. Synthesis and properties of lipoamino acid-fatty acid mixtures: Influence of the amphiphilic structure. *J. Surfactants Deterg.* **2009**, *12*, 269–275. [[CrossRef](#)]
7. Rosen, M.J.; Kunjappu, J.T. *Surfactants and Interfacial Phenomena*; John Wiley & Sons: Hoboken, NJ, USA, 2012; ISBN 9780470541944.
8. Bajani, D.; Gharai, D.; Dey, J. A comparison of the self-assembly behaviour of sodium N-lauroyl sarcosinate and sodium N-lauroyl glycinate surfactants in aqueous and aqueo-organic media. *J. Colloid Interface Sci.* **2018**, *529*, 314–324. [[CrossRef](#)] [[PubMed](#)]
9. Sakamoto, K.; Lochhead, R.Y.; Maibach, H.I.; Yamashita, Y. *Cosmetic Science and Technology: Theoretical Principles and Applications*; Elsevier: Amsterdam, The Netherlands, 2017; ISBN 9780128020548.
10. Macfarlane, M.G. *Phosphatidylglycerols and Lipoamino Acids*; Academic Press Inc.: London, UK, 1964; Volume 2.
11. Nnanna, I.A.J.X. *Protein-Based Surfactants*; Marcel Dekker. Inc.: New York, NY, USA, 2001; ISBN 082470004X.
12. Cartwright, N.J. Serratamic acid, a derivative of L-serine produced by organisms of the Serratia group. *Biochem. J.* **1955**, *60*, 238–242. [[CrossRef](#)]

13. Hell, R. Molecular physiology of plant sulfur metabolism. *Planta* **1997**, *202*, 138–148. [[CrossRef](#)] [[PubMed](#)]
14. Bulaj, G. Formation of disulfide bonds in proteins and peptides. *Biotechnol. Adv.* **2005**, *23*, 87–92. [[CrossRef](#)] [[PubMed](#)]
15. Komarov, P.; Ovchinnikov, M.; Khizhnyak, S.; Alekseev, V.; Mikhailov, I.; Pakhomov, P. On Molecular Gelation Mechanism of L-Cysteine Based Hydrogel. *Nanosci. Nanoeng.* **2013**, *1*, 23–35. [[CrossRef](#)]
16. Dunetz, J.R.; Magano, J.; Weisenburger, G.A. Large-Scale Applications of Amide Coupling Reagents for the Synthesis of Pharmaceuticals. *Org. Process Res. Dev.* **2016**, *20*, 140–177. [[CrossRef](#)]
17. Sheehan, J.C.; Hess, G.P. A new method of forming peptide bonds. *J. Am. Chem. Soc.* **1955**, *77*, 1067–1068. [[CrossRef](#)]
18. Madison, S.A.; Carnali, J.O. PH optimization of amidation via carbodiimides. *Ind. Eng. Chem. Res.* **2013**, *52*, 13547–13555. [[CrossRef](#)]
19. Michael, B.; Smith, J.M. *March's Advanced Organic chemistry: Reactions, Mechanisms, and Structure*; John Wiley & Sons: Hoboken, NJ, USA, 2001.
20. Ullah, I.; Ahmad, K.; Shah, A.; Badshah, A.; Ali Rana, U.; Shakir, I.; Zia-Ur-Rehman, Z.; Khan, S.Z. Synthesis, characterization and effect of a solvent mixture on the CMC of a Thio-based novel cationic surfactant using a uv-visible spectroscopic technique. *J. Surfactants Deterg.* **2014**, *17*, 501–507. [[CrossRef](#)]
21. Rather, M.A.; Rather, G.M.; Pandit, S.A.; Bhat, S.A.; Bhat, M.A. Determination of cmc of imidazolium based surface active ionic liquids through probe-less UV-vis spectrophotometry. *Talanta* **2015**, *131*, 55–58. [[CrossRef](#)] [[PubMed](#)]
22. Jacobsen, N.E. *NMR Data Interpretation Explained: Understanding 1D and 2D NMR Spectra of Organic Compounds and Natural Products*; John Wiley & Sons: Hoboken, NJ, USA, 2017; ISBN 9781118370223.
23. Reich, H.J. Proton Chemical Shifts Database. 2017. Available online: <https://www2.chemistry.msu.edu/faculty/reusch/OrgPage/nmr.htm> (accessed on 13 April 2021).
24. López-Millán, A.; Zavala-Rivera, P.; Esquivel, R.; Carrillo, R.; Alvarez-Ramos, E.; Moreno-Corral, R.; Guzmán-Zamudio, R.; Lucero-Acuña, A. Aqueous-Organic Phase Transfer of Gold and Silver Nanoparticles Using Thiol-Modified Oleic Acid. *Appl. Sci.* **2017**, *7*, 273. [[CrossRef](#)]
25. Cameron, D.G.; Umemura, J.; Wong, P.T.T.; Mantsch, H.H. A fourier transform infrared study of the coagel to micelle transitions of sodium laurate and sodium oleate. *Colloids Surf.* **1982**, *4*, 131–145. [[CrossRef](#)]
26. Yea, D.N.; Lee, S.M.; Jo, S.H.; Yu, H.P.; Lim, J.C. Preparation of Environmentally Friendly Amino Acid-Based Anionic Surfactants and Characterization of Their Interfacial Properties for Detergent Products Formulation. *J. Surfactants Deterg.* **2018**, *21*, 541–552. [[CrossRef](#)]
27. Bellamy, L.J. *The Infrared Spectra of Complex Molecules*, 2nd ed.; Chapman and Hall: London, UK, 1980; Volume 53, ISBN 9788578110796.
28. Cebi, N.; Dogan, C.E.; Develioglu, A.; Yayla, M.E.A.; Sagdic, O. Detection of L-Cysteine in wheat flour by Raman microscopy combined chemometrics of HCA and PCA. *Food Chem.* **2017**, *228*, 116–124. [[CrossRef](#)] [[PubMed](#)]
29. Peter, L. *IR and Raman Spectroscopy*; Elsevier Inc.: San Diego, CA, USA, 2011; Volume 53, ISBN 9780123869845.
30. Suga, K.; Kondo, D.; Otsuka, Y.; Okamoto, Y.; Umakoshi, H. Characterization of Aqueous Oleic Acid/Oleate Dispersions by Fluorescent Probes and Raman Spectroscopy. *Langmuir* **2016**, *32*, 7606–7612. [[CrossRef](#)] [[PubMed](#)]